Design: #1: EAT-susceptible CBA/J mice (8-12 wks) were injected with 40 μg mTg followed 3 hrs later by 10,000 IU rIL-1β (days 0, 7). Sera were obtained on day 14 and thyroids were processed on day 28. **#2**: Mice were depleted of Tregs by injection of CD25 mAb (days -11, -7). Mice were injected with 40 μg mTg followed 3 hrs later by 0.5 μg LPS (day 7), and mTg only (days 14, 21). **#3**: Tregs were depleted by CD25 mAb treatment (days -14, -10). Mice were injected with 16 doses of 40 μg mTg without adjuvant from days 0 to 24 (4X/week). Thyroids and sera were obtained on day 35. All thyroids were examined for cellular infiltration and follicular destruction. Splenocytes were cultured with mTg, and proliferation was assessed by [^{3}H]thymidine uptake. Anti-mTg levels were quantitated by ELISA.
Results: #1: Moderate thyroiditis, T cell proliferation and anti-mTg levels were observed in all mice treated with rIL-1β. **#2:** Treg-depleted mice had higher thyroiditis incidence and severity, increased T cell proliferation and anti-mTg levels, compared to controls. **#3:** Compared to mice given repeated mTg doses only, Treg depletion led to greater thyroiditis incidence and severity, and higher anti-mTg levels.
Conclusions: EAT can be induced in susceptible mice by treatment with mTg and rIL-1β or reduced LPS. The incidence and severity increase with Treg depletion. When repeated mTg doses without adjuvant followed Treg depletion, EAT incidence and severity are also augmented. These protocols will aid the study of consequences of immunotherapy in susceptible patients or those with pre-existing autoimmune thyroid disease. (Supported by St. John Hosp.)

Pediatrics

1705 Morphoproteomics Provides Further Insight into the Biology of Metastatic Osteosarcoma and Identifies Potential Therapeutic Targets.

S Alexandrescu, P Anderson, J Buryanek, RE Brown. University of Texas- Medical School, Houston; MD Anderson Cancer Center, Houston, TX.
Background: Metastasis in osteosarcoma decreases the survival to 10-25%. Establishing a targeted therapeutic protocol for these patients is challenging, because of genetic instability. However, these tumors have common biologic components that might be targets for therapy (expression of c-Met, TRAIL (DR4), and activation of insulin-like growth factor-1 receptor (IGF1R) signaling pathway).
Design: Three consulting pathologists examined tissue from four MD Anderson Cancer Center patients (age range 11-16) with multiple sites of metastatic osteosarcoma unresponsive to treatment. A morphoproteomic analysis of signaling pathways, cell cycle analytes, antiapoptotic/tumorigenic/angiogenic/chemoresistance factors, proapoptotic proteins and stem cell markers was performed.
Results: We observed: variable activation of ras/Raf kinase/extracellular signal regulated-kinase (ERK) pathway, evident by nuclear translocation of p-ERK1/2 (Thr202/Tyr204) in a majority of the tumor cells; activation of the mammalian target of rapamycin (mTOR) pathway in many tumor cells with p-mTOR(Ser 2448) in both cytoplasmic and nuclear compartments (consistent with variable mTORC1 and mTORC2 activation); brisk cell cycle progression;expression of tumorigenic proteins, heat shock protein (Hsp)90, p-p38MAPK (Thr 180/Tyr182)and fatty acid synthase (FAS); proapoptotic TRAIL-DR4 expression; and a CD133 and nestin stem cell immunophenotype. EGFRvIII/wild type, HER-2 and VEGF-A were absent or weakly expressed in a minority of cells.
Conclusions: This consultative study provides an explanation for the limited efficacy of some of the agents used in these patients (bevacizumab, rapamycin, anti-EGFR antibody), and suggests new targeted therapies.Sorafenib and aminobisphosphonates act to downregulate the ras/Raf kinase/ERK pathway. Metformin inhibits IGF-1R signaling pathway at the level of IRS-1, induces TRAIL-mediated apoptosis in osteosarcoma and contributes to cell cycle arrest. It also inhibits fatty acid synthase, representing a convenient substitute for c-MET inhibitor. Doxorubicin sensitizes osteosarcoma cells, but not normal bone cells to Apo2L/TRAIL-induced apoptosis and targets mitotically active tumor. Melatonin inhibits cell cycle progression and augments chemotherapy while minimizing toxic side effects.

1706 Metformin Induces Cell Death in a Human Neuroblastoma Cell Line through Affecting Multiple Survival Pathways.

H Chai, P Weerasinghe, RE Brown. University of Texas- Medical School, Houston.
Background: Neuroblastoma is the most common extracranial solid cancer in childhood. Its tumorigenicity is enhanced by the expression of survival pathways such as Akt and signal transducer and activator of transcription (STAT)3 as well as an inappropriate level of mammalian target of rapamycin (mTOR) activity. Metformin is one of the most widely used diabetes drugs. It has shown inhibiting effects on mTOR, which may prevent the growth of cancer cells. In this study, we will examine the efficacy of metformin on a human neuroblastoma cell line and also investigate its possible mechanisms.
Design: A neuroblastoma cell line, SK-N-AS, was purchased from ATCC. After reaching 50-60% confluence, cells were treated with various concentrations of metformin (0, 1, 5, 10, 20, 40 mM) for different period of times (0, 30 min, 2, 6, 24, 48 and 72 hours). The cell viability was determined by MTT colorimetric assay. The apoptotic responses were measured with TUNEL assay. Phosphorylation of Akt1/2/3 (p-Akt1/2/3 [Thr308]), AMP-activated protein kinase alpha1 subunit (p-AMPKa1 [Thr172]), p42 MAP Kinase (p-ERK2), STAT3 (p-STAT3 [Ser727]), and mTOR (p-mTOR [S2448]) and total mTOR (mTOR [7C10]) protein expression levels were determined with Western blot assay.
Results: As early as 6 hours post-treatment, cell viability was significantly decreased at 10 mM concentration. In 24 and 48 hours treatment groups, metformin at 5 mM and above concentrations significant decreased cell viability. TUNEL assay showed similar results. Western blots showed a decrease of p-Akt2 and p-STAT3 expression levels in metformin treatment groups. An increase of p-ERK2, p-AMPKa1 was also observed. Total mTOR levels were slight increased while the phosphorylation at S2448 site was significantly decreased.
Conclusions: Our results indicate that metformin significantly decreased cell viability and increased cell death in a human neuroblastoma cell line in association with down-regulation of p-Akt, p-STAT3 and p-mTOR survival pathways. These data suggested a potential clinical application of metformin in the treatment of neuroblastoma cases with constitutive activation of Akt, STAT3 and mTOR.

1707 β-Catenin and Novel Associated Proteins in Nasopharyngeal Angiofibromas.

SL Cook, RD LeGallo, SE Mills, EB Stelow. University of Virginia, Charlottesville.
Background: Nasopharyngeal angiofibromas occur at an increased frequency in patients with familial adenomatous polyposis. Furthermore, a majority of sporadic nasopharyngeal angiofibromas has been shown to have nuclear accumulation of β-catenin and have mutations in the β-catenin gene. These results suggest that the Wnt-signaling pathway is important in the pathogenesis of both sporadic and syndrome-associated tumors. End-binding protein 1 (EB1) is an adenomatous polyposis coli (APC)-binding protein which associates with growing ends of microtubules and has been reported to be overexpressed in some carcinomas. Cyclin D1 is a transcriptional target of β-catenin which promotes cell cycle progression. While WT1 functions in transcription regulation, it is now speculated that it also plays a role as a tumor suppressor of the Wnt-signaling pathway. Here, we examine the expression patterns of β-catenin, EB1, cyclin D1, and WT1 in a series of nasopharyngeal angiofibromas.
Design: The study examined 14 nasopharyngeal angiofibromas resected from 14 males ranging in age from 10 to 23 years and found within the surgical pathology files of a single institution. Immunohistochemistry was performed for β-catenin, EB1, cyclin D1, and WT1. Staining pattern and characteristics and the percentage of cells staining were recorded.
Results: All fourteen nasopharyngeal angiofibromas showed prominent nuclear accumulation of β-catenin. In addition, 13 of 13 showed strong, granular cytoplasmic accumulation of EB1. Cyclin D1 showed nuclear staining in a minority of cells (<10% of cells) in 9 of 14 cases. All fourteen tumors showed cytoplasmic staining with WT1. In 7 of 14 (50%) of cases, cytoplasmic WT1 was present in 20 to 50% of cells, while the remaining 7 cases had staining in 70 to 90% of cells.
Conclusions: We confirm the strong and diffuse nuclear accumulation of β-catenin in nasopharyngeal angiofibromas previously noted by others. Cyclin D1 staining supports the functional status of the activated β-catenin. Interestingly, the expression of the novel protein EB1 suggests a role for APC in these tumors. Also, the expression of WT1 in these tumors known to have β-catenin accumulation provides further evidence of its role as a potential tumor suppressor of the Wnt-signaling pathway. Aside from providing information regarding the pathobiology of these tumors, these results also suggest a possible use for these immunostains in the diagnosis of these tumors.

1708 Intratubular Germ Cell Neoplasia, Unclassified Type (IGCNU), in Prepubertal, Cryptorchid Testes: A 20 Year Experience at a Major Pediatric Hospital.

R Fan, TM Ulbright. Indiana University, Indianapolis.
Background: Maldescended testes frequently come to the attention of pathologists, especially in pediatric hospitals. It remains controversial if prepubertal testes develop IGCNU. We therefore reviewed our experience over a 20-year interval with maldescended, prepubertal testes that carried a diagnosis of IGCNU.
Design: With approval of the Institutional Review Board, we performed several searches in our computerized pathology database from January 1990 to December 2009 to identify all testicular and paratesticular lesions. Next we examined all cases carrying a diagnosis of IGCNU. All were in maldescended testes.
Results: Of 883 testicular and paratesticular specimens, 276 represented atrophy/cryptorchidism (236) or intersex disorders (40). Among these 276 specimens, 6 from 5 patients with cryptorchidism carried a diagnosis of atypical intratubular germ cells. Three patients had a known intersex disorder and, on review, the specimens met the morphological and immunohistochemical criteria for IGCNU. Review of the remaining 3 specimens from 2 patients, who lacked an established diagnosis of an intersex disorder, verified that the atypical germ cells in 1 case lacked the features of IGCNU but showed nuclear enlargement with hyperchromasia and frequent central position within the tubules; these cells did express fetal germ cell markers (OCT3/4, placental alkaline phosphatase, CD117) also expressed in IGCNU and likely reflect delayed germ cell maturation, as has been described in the gonads of patients with undervirilization syndromes. The last patient, who was not known to have an intersex disorder, had a right duplex dysplastic kidney with both upper and lower pole obstruction and bilateral undescended testes. Review of his testicular specimens obtained at 9 weeks and 4 months, showed dysgenetic features, with ovarian type stroma and malformed tubules as well as IGCNU. We therefore consider him to have a previously undiagnosed intersex disorder, a conclusion also supported by the surgeon's intraoperative impression. We therefore did not identify a bona fide case of IGCNU in prepubertal maldescended testes outside of a known intersex disorder or with findings highly suggestive of one.
Conclusions: Based on our experience it is questionable if legitimate examples of IGCNU occur in prepubertal testes apart from an intersex disorder. Careful morphological and immunohistochemical evaluation and correlation with clinical findings are essential in the examination of prepubertal cryptorchid testes to avoid overdiagnosing IGCNU.

1709 Correlation between Vascular Endothelial Growth Factors Expression and Risk of Bone Marrow Metastasis in Children with Neuroblastoma.

K Hooper, AG Saad, JM Osman. Arkansas Children's Hospital, Little Rock.

Background: Neuroblastoma (NB) is a common pediatric neoplasm. Histopathological features remain a poor predictor of the risk of developing distant metastases, in particular bone marrow (BM) metastasis, in patients with NB. Despite significant advances in therapeutic protocols, the prognosis of children with NB remains largely poor. We conducted this study to investigate the correlation between the expression of various VEGFs in NB and the development of BM metastasis.

Design: Twelve patients (group 1) with NB and BM metastasis and 9 patients (group 2) with negative BM are included in this study. Slides from the primary tumor are immunostained with antibodies against VEGFR-1, VEGFR-2, VEGF-B, and VEGF-D. Each slide is scanned and the percentage of VEGF-positive blood vessels in the tumor is estimated using semi-quantitative method. The expression of each VEGF is correlated with the risk of developing BM metastasis.

Results: Group 1 (mean age 20.6 months; range 0.5-61 months) consisted of 7 males and 5 females. Group 2 (mean age 67.8 months; range 24-156 months) consisted of 3 males and 4 females. There was a statistical difference in the expression of VEGFR-1 and VEGF-B between both groups (P=0.02 and 3.04E-05, respectively). We observed no significant difference in the expression of VEGFR-2 between both groups (P=0.19). There was complete absence of expression of VEGF-D in both groups of patients. A significantly increased risk of BM metastasis was found in patients with high expression of VEGFR-1 and VEGF-B. It appears that VEGF-D plays no role in angiogenesis or tumor progression of NB. Details of the expression of various VEGF inlcuded in this study are summarized in table 1.

Table 1-VEGF expression in neuroblastoma

Neuroblastoma	VEGFR-1		VEGFR-2		VEGF-B	
	Mean	Range	Mean	Range	Mean	Range
With BM metastasis	38.3	10-80	56	2-100	84	70-90
Without BM metastasis	12.5	0-50	68.9	50-100	36	10-60

Conclusions: Our study indicates that patients with neuroblastoma with high expression of VEGFR-1 and VEGF-B in their primary tumors have a greater risk of developing bone marrow metastasis. Our study suggests that patients with neuroblastoma and a specific biomarker expression may benefit from an individualized surveillance regimen and a preventive therapeutic intervention designed to prevent of delay the development of bone marrow metastasis. This preliminary study provides a promising tool that may help in the management of neuroblastoma patients in particular treatment with anti-VEGF targeted therapy.

1710 DICER1 Mutations in Familial PPB-Tumor Predisposition Syndrome-Associated and Sporadic Rhabdomyosarcomas.

JA Jarzembowski, L Doros, DA Hill, J Yang, K Skiver, YH Messinger, G Williams, LP Dehner. Children's Hospital of Wisconsin, Milwaukee; Children's National Medical Center, Washington, DC; The International Pleuropulmonary Blastoma Registry, Minneapolis, MN; Washington University in St. Louis, MO.

Background: Pleuropulmonary blastoma (PPB), a rare dysontogenic tumor of the lung, appears to arise as a perturbation in the branching morphogenetic phase of lung development with the added capacity for malignant progression. This initial multicystic lesion is accompanied by a primitive population of cells with or without an embryonal rhabdomyosarcoma [ERMS]-like component. We recently discovered that patients with a familial PPB-tumor predisposition have germline loss-of-function mutations in *DICER1*, an miRNA processing enzyme which helps orchestrate organogenesis. We have also observed that some ERMS, especially those of the uterine cervix, resemble PPB with cartilaginous nodules and septated cysts. Because of the histologic overlap between PPB and ERMS and their co-occurrence in some syndromic families we investigated the role of *DICER1* in ERMS.

Design: Three probands and one uncle from PPB syndromic families were diagnosed with extrathoracic RMS (1 uterine cervix, 3 bladder). Germline DNA from these cases along with tumor DNA from an additional 52 ERMS obtained from the Cooperative Human Tissue Network (CHTN) archive were analyzed for *DICER1* mutations by directly sequencing all coding exons and flanking sequences.

Results: All 4 ERMS in PPB families had loss of function *DICER1* mutations: 2 were nonsense mutations and 2 were insertion/deletion variants. Of the 52 ERMS without PPB syndrome, 2 had *DICER1* mutations: 1 insertion/deletion and 1 splice junction mutation. All 6 mutations are predicted to result in loss of functional DICER1 from this allele.

Conclusions: Our findings suggest that a small but significant fraction (4%) of pediatric ERMS harbor *DICER1* mutations, suggesting a role for miRNAs in the pathogenesis of these tumors. Germline DNA from most cases was not available, and we cannot determine whether the mutations are tumor-specific or germline. Inherited germline mutations are found in the majority of children with PPB, most of whom show no other signs of the familial PPB-tumor syndrome. It will be important to know if patients with "sporadic" ERMS have germline mutations because then they, their progeny, and their family members are potentially at risk for developing PPB and other malignancies and should be counseled.

1711 Nephrogenic Adenomas in Pediatric Patients: An Immunophenotypic Study and Ten-Year Institutional Experience.

JB Kum, R Fan, JN Eble, M Idrees. Indiana University, Indianapolis.

Background: In children, nephrogenic adenomas are rare benign lesions that often occur in the setting of previous surgery or chronic irritation of the urinary tract. The exact pathogenesis of nephrogenic adenoma is unknown. There is recent convincing evidence that nephrogenic adenomas are derived from renal tubular cells that are shed, migrate, reimplant and proliferate within urothelial mucosa. These lesions often present with hematuria and/or polypoid mass on cystoscopy. They frequently reoccur and can be symptomatic. We sought to evaluate the immunophenotype of these lesions in the pediatric population.

Design: We examined 20 cases of nephrogenic adenoma diagnosed from urinary bladder biopsies in 15 patients. Biopsies were obtained between 2000 and 2010. Immunohistochemistry stains for cytokeratin 7, P504S, Pax-2, Pax-5, CD10, p63 and MUC-1 (enzyme conjugated polymer visualization system) were performed. The immunohistochemistry stains for each antibody were graded for intensity on a scale from 0-3 and for extent of staining ranging from focal (0-10% of cells), partial (10-50% of cells) to diffuse (50-100% of cells).

Results: The age range was 2 to 18 years old (mean 10 years old). Nine occurred in males and 11 in females. Seven of the cases occurred in patients with history of bladder augmentation, two in patients with history of bladder stones, 1 case in a patient with history of urinary tract infection and the remaining 5 cases in patients who had other urinary bladder surgery. Strong and diffuse staining was observed with cytokeratin 7 (cytoplasmic) and MUC-1 (luminal) in all cases (100%). Strong diffuse staining was observed with Pax-2 (nuclear) in 17 of 20 cases (85%). p63 and Pax-5 did not stain any of the cases (0%). Variable staining was observed with P504S and ranged from negative (4), focal 1+ staining (9) to diffuse (7). Variable staining was also observed with CD10 and ranged from negative (2), focal 1+ staining (9) to diffuse (9). The adjacent urothelium showed a consistent immunoprofile of cytokeratin 7 and p63 reactivity and no reactivity for P504S, Pax-2, Pax-5, CD10, and MUC-1.

Conclusions: In pediatric patients, nephrogenic adenoma although rare, should be included in the differential diagnosis of polypoid lesions in the urinary tract especially in the context of previous surgery. The immunohistochemistry profile of nephrogenic adenomas in our study provides evidence that nephrogenic adenomas in pediatric patients are derived from distal renal tubular cells. In difficult cases, we recommend an immunohistochemistry panel including cytokeratin 7, p63, Pax-2 and MUC-1.

1712 miR-17-5b Inhibition Decreases Rhabdomyosarcoma Cell Growth In Vitro.

C Liu, S Galli, M Tsokos. NCI/NIH, Bethesda, MD.

Background: microRNAs have been recognized as important players in tumorigenesis. One of these microRNAs, the cluster miR-17-92, exhibits potent oncogenic activity in many tumors. A recent study demonstrated overexpression of miR-17-92 in rhabdomyosarcoma, but its exact role in this tumor has not been clarified. Rhabdomyosarcoma is the most common soft tissue sarcoma in children and young adults. Even with aggressive therapy, many patients with rhabdomyosarcoma show poor clinical outcome. Investigation of tumorigenic pathways, such as that of the oncogenic miR-17-92 cluster, may lead to identification of novel therapeutic targets. Here we report that inhibition of miR-17-5b, one component of the oncogenic microRNA cluster, decreases rhabdomyosarcoma cell growth in vitro.

Design: Four rhabomyosarcoma cell lines were used: two (Rh4 and Rh28) alveolar and two (Rh36 and CTR) embryonal. The miR-17-5b miRIDIAN Hairpin Inhibitor was transfected with Lipofectamin 2000 to inhibit the function of endogenous miR-17-5b. Cell proliferation was measured using an assay that detected cellular dehydrogenase activity (CCK-8 kit) over a period of five days. Transfected cells were stained with propidium iodide and analyzed for cell cycle arrest using flow cytometry. Real-time RT-PCR and Western blotting were performed to evaluate the expression levels of genes that were involved in cell cycle arrest and apoptosis.

Results: Five days after transfection with the miR-17-5b inhibitor, all four rhabdomyosarcoma cell lines showed decreased cell proliferation. Flow cytometry demonstrated moderate increase in the percentage of G0/G1 arrested cells. p21, a key regulator of G0/G1 cell cycle arrest, was upregulated. BIM, an important proapoptotic protein in mitochondria-mediated apoptosis, was upregulated as well. These findings suggest that miR-17-5b promotes a malignant phenotype in rhabdomyosarcoma through p21-mediated cell cycle deregulation and BIM-mediated inhibition of apoptosis.

Conclusions: Our data show that miR-17-5b inhibition in rhabdomyosarcoma cells causes significant decrease in cell proliferation, promotes moderate cell cycle arrest and induces apoptotic pathways. Therefore, miR-17-5b may play an important role in the tumorigenesis of rhabdomyosarcoma and may serve as a potential therapeutic target for this tumor.

1713 Vinculin-ALK Oncoprotein in a Pediatric Renal Medullary Carcinoma: Rapid Identification by Proteomic Methods.

A Marino-Enriquez, W-B Ou, CB Weldon, JA Fletcher, AR Perez-Atayde. Brigham and Women's Hospital, Boston, MA; Harvard Medical School, Boston, MA; Children's Hospital Boston, MA.

Background: Renal Medullary Carcinoma (RMC) is an aggressive malignancy that affects young black individuals with sickle cell trait. Little is known about RMC pathogenesis, there are no effective drug treatments, and average overall survival is <4 months. ALK is a druggable receptor tyrosine kinase, which is activated oncogenically in subsets of inflammatory myofibroblastic tumor, neuroblastoma, atypical large cell lymphoma and lung adenocarcinoma. Proteomic approaches have not been used previously to identify novel fusion oncogenes.

Design: Cytogenetic analysis of a pediatric RMC revealed a novel t(2;10) translocation involving the *ALK* gene region. A mass-spectrometry based proteomic strategy was used to rapidly characterize the putative ALK fusion partner.

Results: The patient was a 6 year-old black boy with sickle cell trait presenting with a 4.6 cm mass centered in the renal medulla. Histopathologically, the tumor consisted of sheets of polygonal to spindle shaped cells with large vesicular nuclei, clear coarse chromatin and abundant eosinophilic cytoplasm with frequent intracytoplasmic lumens, which ultrastructurally were lined by well-formed microvilli. Focal stromal desmoplasia

and a diffuse lymphoplasmacytic infiltrate were present, as well as prominent vascular invasion of the renal sinus. Tumor cells were immunoreactive for cytokeratins and EMA. INI-1 nuclear expression was retained. The abnormal karyoptype was: 46,XY,t(2;10)(p23;q22),add(14)(p11), with involvement of the *ALK* gene region at 2p23. Dual-color FISH demonstrated *ALK* rearrangement, and strong ALK expression was shown by immunohistochemistry. ALK immunoprecipitation, coupled with phosphotyrosine immunoblotting, identified a strongly activated and aberrantly sized (160kDa) ALK protein. Mass spectrometry revealed this to be a vinculin-ALK fusion protein, in which the N-terminal aspect of vinculin was fused to the ALK kinase domain. These studies also demonstrated a potential mechanism of oncogenic ALK activation, mediated by vinculin interactions with talins.

Conclusions: We present a pediatric RMC harboring a novel *ALK* rearrangement. This study broadens the spectrum of ALK-related tumors and ALK fusion partners, provides insight into RMC pathogenesis, and establishes a biological rationale for targeted kinase-inhibitor therapeutics in this highly lethal disease.

1714 Kidney Injury Molecule-1 Staining Identifies Acute Tubular Injury in Pediatric Kidneys Regardless of Autolysis.

ME Pietrangelo, JK Macknis, SK Hicks, PL Zhang. William Beaumont Hospital, Royal Oak, MI.

Background: Kidney injury molecule-1 (KIM-1) is a specific marker for identifiying injury in proximal tubules. Our recent study demonstrates that KIM-1 is expressed in injured proximal tubules in adult kidneys regardless of autolysis and is significantly associated with premortem serum creatinine (sCr). The current study was to identify proximal tubular injury in kidneys from pediatric autopsies using KIM-1. The second goal was to determine the correlation between clinical indices and KIM-1 expression, since sCr was not available in this age group.

Design: Pediatric autopsy cases (n=52) were identified in our archives from 1/08 to 6/10. All pediatric kidney sections were stained by a Dako Autostainer using a KIM-1 antibody (AKG7, JV Bonventre's lab, Brigham and Women's Hospital, Boston). The staining intensity of KIM-1 in proximal tubules was scored from 0 (no staining) to 3+ (strong granular staining across the entire luminal surface). The autolysis was graded from 0 (no autolysis) to 3+ (entire loss of chromatin staining). The presence of aspirated amniotic fluid contents in stillborn or need for intubation in liveborn were obtained as indices of hypoxia and correlated with KIM-1 expression.

Results: In our pediatric cases, the ages ranged from 15 to 40 gestational weeks (n=52, 29/52 stillborn and 23/52 liveborn). KIM-1 was expressed in 40/52 (77%) of cases: 0 expression in 12 cases; 1+ in 25 cases; 2+ in 14 cases and 3+ in 1 case. KIM-1 staining was upregulated as early as 16 weeks gestation. Twenty-three (23) cases did not show autolysis, whereas autolysis was present in twenty-nine (29) kidneys ranging from 1+ in 8 cases, to 2+ in 7 cases, and to 3+ in 14 cases. There was no significant correlation between KIM-1 scores and autolysis scores (r value = 0.201 and p = 0.1521, linear regression analysis). Cinical correlation (CC) was available for 30/52 (58%) of cases. Among the 30 cases with CC available, there was 73% correlation between KIM-1 expression and either presence of aspirated amniotic fluid contents or need for intubation.

Table 1	Stillborn (%)	Liveborn (%)	Total (%)
KIM-1 +/case #	21/29 (72%)	19/23 (83%)	40/52 (77%)
CC available/case #	11/29 (38%)	19/23 (83%)	30/52 (58%)
CC +/KIM-1 +	6/11 (55%)	16/19 (84%)	22/30 (73%)

Conclusions: Our data suggest that proximal tubular injury in pediatric kidneys can be identified by KIM-1 staining regardless of autolysis. Finding 73% correlation between KIM-1 expression and abnormal clinical indices implies that KIM-1 may be a reliable marker to indicate hypoxic state in pediatric autopsies.

1715 Congenital Pulmonary Airway Malformation: 24 Cases from a Tertiary Referral Center.

DM Reddi, EN Pavlisko, JL Burchette, TA Sporn, VL Roggli. Duke University Medical Center, Durham, NC.

Background: Congenital pulmonary airway malformation (CPAM), formerly known as congenital cystic adenomatoid malformation (CCAM) is a rare congenital cystic pulmonary lesion, secondary to abnormal embryogenesis with anomalous lung and airway development. Several have hypothesized that CPAM subtypes originate at distinct stages of lung development with bronchiolar subtypes (CPAM types I to III) developing in the pseudoglandular stage and the acinar-alveolar subtype (CPAM type IV) occurring in late saccular period. Increased E-cadherin, which is regulated by HOXb5, is seen in CPAM lesions. Here we report, CPAM frequency and associated congenital anomalies in a tertiary referral center. We further hope to elucidate E-cadherin protein expression in specific CPAM types.

Design: With institutional approval, 24 cases (21 surgical; 3 autopsy) of CCAM/CPAM from 1993 to 2010 and age-matched controls were retrieved from our archives for clinicopathologic correlation. E-cadherin expression by immunohistochemistry was evaluated in representative cases from types I to III and compared to age-matched controls.

Results: Of 24 cases (13 male; 12 female) patient age at radiographic diagnosis ranged from 5.5 weeks gestation to 47 years; pathologic confirmation ranged from 24 weeks gestation to 47 years. Frequency of CPAM types I to III was 50%, 37.5% and 12.5%, respectively. The right lung was more often affected, with lower lobe predominance. Additional congenital anomalies were localized to the thoracic cavity and included extrapulmonary sequestration, bronchogenic cyst, diaphragmatic hernia and pulmonary hypoplasia. One case of bronchiolo-alveolar cell carcinoma arose from CPAM type I. In comparison to age-matched controls, E-cadherin protein expression, as qualified by immunohistochemistry, is uniformly strongly expressed in representative CPAM types I to III in comparison to controls.

Conclusions: The most common type of CPAM is type I. Although congenital anomalies, notably extrapulmonary manifestations, have been associated with type II, our cases show congenital anomalies in other types. Radiographic diagnosis of type I occurred as early as 5-6 weeks which indicates that the bronchiolar subtype may develop in or prior to the pseudoglandular stage. HOXb5 upregulation has been previously reported in CPAM without specification to type. Our series indicates increased E-cadherin protein expression via immunohistochemistry specifically in the bronchiolar subtype which may correlate with increased gene expression and upregulation of the HOXb5 pathway.

1716 Expression of Notch Pathway Components in Wilms' Tumour.

R Santi, M Paglierani, M Pepi, D Massi, G Nesi. University of Florence, Italy.

Background: Wilms' tumour (nephroblastoma) is the most common kidney cancer in childhood. It derives from embryonic renal precursors and is often associated with lasting embryonic renal tissue. Notch signalling plays a crucial role in many developmental processes and may contribute to oncogenesis in a tissue-specific manner. Recent studies document the expression of Notch pathway proteins during nephrogenesis. The aim of this study was to investigate the expression and patterning of Notch pathway components in a series of Wilms' tumours.

Design: Fourteen primary nephroblastomas and five nephroblastoma metastases to the lung were reviewed on haematoxylin-eosin stained slides. Notch-1 and Notch-2 protein expression was studied by immunohistochemical assay. Tissue sections were labelled with the following antibodies: goat anti-human Notch-1 (sc-6014) and goat anti-human Notch-2 (sc-5545) (Santa Cruz Biotechnology Inc.).

Results: There were 10 females and 6 males, ranging from six months to 34 years of age. On light microscopy, the surgical specimens harboured triphasic (n=7; 36%), biphasic (n=6; 32%) or monophasic (n=6; 32%) lesions. Among the 14 cases displaying an epithelial component, Notch-2 immunostaining was detected in 10 (71%), whereas only in 3/17 (18%) cases blastema showed faint and focal Notch-2 reactivity. The stromal component showed variable degrees of Notch-2 immunoreactivity with a higher intensity in tumours exhibiting myogenic features. In all cases, normal renal tissue and vascular endothelial cells were strongly and diffusely positive for Notch-2. Notch-1 expression substantially overlapped Notch-2 immunohistochemical results, although with a lower intensity of staining.

Conclusions: Preliminary results of this study indicate a decreased expression of Notch-2 and Notch-1 proteins in the blastema, when compared with the epithelial and the myogenic components or the peritumoral renal parenchyma. Further studies are needed to better assess the role of Notch signalling in nephroblastoma oncogenesis and its putative interactions with pathways involved in tumour progression and invasiveness.

1717 Biliary Dyskinesia in Children: A Mast Cell-Related Disorder?

SG Sharma, AG Saad. University of Arkansas for Medical Sciences, Little Rock; Arkansas Children's Hospital, Little Rock.

Background: Studies suggest a close association between mucosal mast cells (MCs) and nerve endings. Biliary dyskinesia (BD) is a common cause of abdominal pain in children, treated with cholecystectomy. Slow gallbladder emptying is implicated as a key pathologic factor in patients with BD. We noticed increased number of MCs in the gallbladder of BD patients. This study evaluates the number of MCs in these gallbladders.

Design: The files were searched for patients with BD from 1985 to 2010. These were compared to a similar number of patients with cholelithiasis (CL). The control group was gallbladders from autopsies with no history of hepatobiliary disorder. Sections were immunostained with monoclonal mouse antihuman mast cells tryptase (clone AA1, Dako).The highest number of MCs were determined in five fields (400x) by manual count, aided by digital imaging in the lamina propria(LP) and muscularis mucosae (MM). Statistical analysis was performed using GraphPad Software (La Jolla, CA).

Results: The search resulted in 29 patients (mean age: 14.1 ± 3.8 years) with BD which were compared with 29 cholelithiasis patients (mean age: 11.4 ± 3.3 years) and 20 control patients (mean age: 10.7 ± 4.2 years). There was no statistically significant difference in age between three groups. Summary of the number and distribution of MCs is shown in Table 1.

Comparison of mast cell density between patients with biliary dyskinesia, cholelithiasis, and controls

	Biliary dyskinesia	Cholelithiasis	Controls
Age (years)	14.1 ± 3.8	11.4 ± 3.3	10.7 ± 4.2
Lamina propria	15.5 ± 6.2	6.9 ± 2.0	2.3 ± 1.4
Muscularis mucosa	12.8 ± 3.9	5.5 ± 1.6	1.8 ± 0.7

Numbers represent mean ± standard deviation

Patients with CL showed more MCs in LP and MM than the controls group; however, difference was not statistically significant. Patients with BD showed statistically significant increase in the number of MCs in LP and MM compared to patients with CL (P-value 2.02E-08 and 2.4E-11, respectively) and the control group (P-value 1.07E-12 and 7.75E-16, respectively).

Conclusions: The results show a marked increase in the number of MCs in the gallbladder of patients with BD as compared to patients with cholelithiasis and to normal gallbladder. Since numerous studies suggest an association between MCs and nerve twigs in the wall of various parts of the gastrointestinal system, our results suggest a pivotal role of MCs in biliary dyskinesia pathogenesis. Further investigations will develop more effective therapeutic approach for these patients.

1718 Fluorescent In Situ Hybridization (FISH) Is an Effective Tool To Detect Unsuspected Trisomies in Hydropic Gestation.

RF Siddiqui, K Chun, Z Ghorab, N Ismiil, MA Khalifa, S Nofech-Mozes, R Osborne, RS Saad, C Sherman, V Dube. Sunnybrook HSC, University of Toronto, ON, Canada; North York General Hospital, Toronto, ON, Canada.

Background: Histological classification of products of conception (POC) with hydropic changes has always been challenging because there is considerable morphological overlap between gestations with hydropic degeneration (HD), partial moles (PM) and hydropic changes due to trisomies. Ancillary studies are essential in establishing diagnosis and flow cytometry has been considered the gold standard to identify triploidy confirming the diagnosis of PM. Fluorescent In situ Hybridization (FISH) is a molecular cytogenetic technique that has been used more recently to identify triploidy in POCs and due to the use of chromosome-specific probes, FISH can also detect specific trisomies. The aim of our study was to assess the efficacy of FISH as a novel ancillary technique in identifying trisomies in POCs with hydropic changes.

Design: The study cohort consists of 67 cases of POC accessionned between 2007 and 2010 for which the differential diagnoses included PM and HD and for which FISH had been requested. FISH was performed on 4-µm formalin-fixed paraffin-embedded tissue sections using the Vysis AneuVysion Prenatal Test specific for chromosomes X, Y, 13, 18 and 21, and a probe specific for chromosome 16 (Abbott-Molecular).

Results: FISH revealed an unsuspected trisomy in 6/67 cases (9%). There were four cases of trisomy 16, one trisomy 18 and one trisomy 21. FISH revealed triploidy confirming a diagnosis of PM in 32/67 cases. In the remaining cases, the FISH results were within normal range and a diagnosis of HD was rendered.

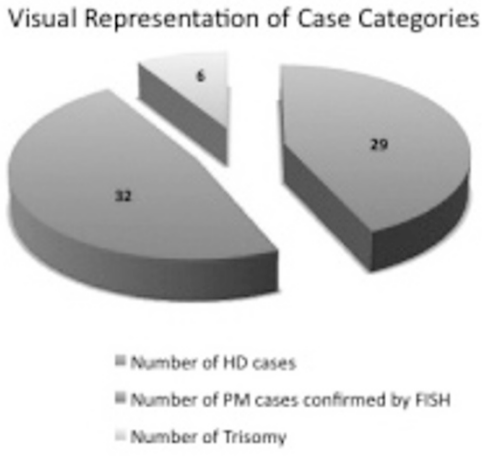

Conclusions: Thus FISH has emerged as an effective tool in not only the definitive diagnosis of PM, but also detection of trisomies in HD cases and the discernment of the cause of the miscarriage. In our study, an unsuspected trisomy was identified in a significant proportion (9%) of POCs with hydropic changes submitted for FISH analysis. A diagnosis of gestation with a trisomy can have significant clinical implications. Thus, FISH, rather than flow cytometry, should be considered as the new gold standard for the evaluation of hydropic POCs.

Pulmonary

1719 The Impact of Pleural Invasion and Its Subdivision on T Staging of Non-Small Cell Lung Cancer.

K Aboualfa, E Lim, P Goldstraw, M Dusmet, G Ladas, S Jordan, AG Nicholson. Royal Brompton and Harefield NHS Foundation Trust, London, United Kingdom; Imperial College, London, United Kingdom.

Background: Visceral pleural invasion (VPI) is a factor that upstages T1 tumours to T2 in the 7th TNM for non-small cell lung carcinoma (NSCLC). However. the value of further subdivision of VPI is controversial. This study assesses the significance of VPI on survival and the value of splitting pleural invasion into further subgroups.

Design: Histopathological data was prospectively collected on 728 resected NSCLCs between 1999 and 2006, according to the RCPathology Minimum Data Set, of which 465 had overall survival data (OS) and 455 had disease free survival data (DFS). Pleural invasion was assessed by using haematoxylin and eosin (H&E) staining and Elastin van Gieson (EVG) staining to highlight the pleura. Pleural invasion was further subclassified according to proposed criteria for PL0 (no VPI), PL1 (VPI not reaching the surface), PL2 (VPI reaching the surface), PL3. (parietal pleural invasion). To assess VPI as an independent variable, T category based purely on size was also documented without contribution of VPI. Actuarial survival was estimated using the Kaplan-Meier method and compared using the Log-rank test. Cox proportional hazards regression was used to ascertain the individual contribution of factors associated with survival and to compare adjusted survival between the groups.

Results: The presence of visceral pleural invasion was associated with a hazard ratio of 1.57 (95%CI 1.19 to 2.11; P=0.001) and 1.49 (1.11 to 2.01; P=0.007), adding 56% and 49% to the mortality at each stage, for the 6th and 7th edition of the TNM respectively, in relation to OS. There was no evidence to suggest any difference in overall (P=0.262) or disease free survival (P=0.183) between the PL1-3 categories.

Conclusions: We confirm the importance of tumour breaching the outer elastin layer of the visceral pleura (VPI) as a signifcant factor in T staging, independent of tumour size. However our data do not support further subdivision of pleural invasion into PL1-3 subcategories.

1720 Detection and Clinicopathologic Features of ALK Rearranged Lung Adenocarcinoma.

DC Ang, JM Reinersman, SC Jhanwar, W Travis, M Ladanyi. Memorial Sloan-Kettering Cancer Center, New York, NY.

Background: The *EML4-ALK* fusion in lung adenocarcinomas (AD) is mutually exclusive with *EGFR* and *KRAS* mutations and is associated with striking responses to ALK kinase inhibitors. The optimal detection strategy and morphologic features of this genetic subset of lung AD remain poorly defined. We compared *ALK* fusion detection by fluorescence in situ hybridization (FISH), immunohistochemistry (IHC), and reverse transcriptase-polymerase chain reaction (RT-PCR), and then used this highly validated set of cases to examine the clinicopathologic features of ALK-rearranged (ALK-R) tumors.

Design: We screened 622 *EGFR* and *KRAS* wild type lung AD for *ALK* rearrangement by dual color split signal FISH assay (Abbott-Vysis; positivity defined as presence of split signals or loss of 5' ALK probe in >5% of tumor cells); 32 *ALK*-R and 99 *ALK*-germline (ALK-G) tumors were then tested by IHC [ALK D5F3 monoclonal antibody, Cell Signaling; scored as negative (0-1+) and positive (2-3+)], and RT-PCR (using 6 *EML4* forward primers; 1 *ALK* reverse primer).

Results: Of the 622 cases tested by FISH, 48 (8%) cases were *ALK*-R and 571 (92%) were *ALK-G*. As *EGFR*- and *KRAS*-germline cases make up about 55% of lung AD in our population, we estimate a 4% overall prevalence of *ALK* fusion. The most common predominant histology was solid (54%), followed by acinar (17%) and papillary (Pap 8%). Signet ring cells were identified in 7 cases (15%) including solid (n=5), Pap (n=1) and Micropapillary (MP, n=1) subtypes. *ALK*-R tumors were strongly associated with non-smokers, solid-predominant histology and high stage (IIIB-IV) at presentation. The concordance rate of IHC and RT-PCR assay with FISH were 97% (77/79; k=0.95) and 95% (131/138; k=0.88), respectively. All 99 *ALK*-G tumors by FISH were negative by IHC and RT-PCR.

Conclusions: Our study suggests that FISH should be combined with IHC as a screening strategy for *ALK* fusions in routine practice, with confirmation by RT-PCR as needed. IHC can raise diagnostic accuracy in cases with low % of FISH-positive cells (5-15%). All FISH-positive cases in this low range were confirmed by IHC/RT-PCR. ALK-R tumors are associated with poorly differentiated lung AD (solid, MP). However, signet ring cells are identified in only 15% of ALK-R tumors.

Clinical features of ALK-R and ALK-G Lung AD

	ALK-R (n=48)	ALK-G (n=99)	P value
Age (median)	31-84 (58)	35-87 (63)	
Female	21 (44%)	60 (61%)	0.1029
Male	27 (56%)	35 (39%)	
Non-Smoker	40 (83%)	21 (21%)	<0.0001
Smoker	8 (17%)	78 (79%)	
Stage IA-IIIA	12 (25%)	67 (68%)	<0.0001
Stage IV	36 (75%)	32 (32%)	

1721 Comprehensive Analysis for Clinically Relevant Oncogenic Driver Mutations in 1131 Consecutive Lung Adenocarcinomas.

ME Arcila, C Lau, S Jhanwar, MF Zakowski, MG Kris, M Ladanyi. Memorial Sloan Kettering Cancer Center, New York, NY.

Background: Somatic mutations within several signaling molecules of the EGFR pathway have been shown to drive lung adenocarcinoma. With the advent of targeted therapies, the prospective assessment of tumors for a growing number of clinically relevant genetic alterations is becoming necessary. In this study, we aimed to determine the proportion of lung adenocarcinomas with known mutations based on a comprehensive panel interrogating 38 mutations in 8 genes.

Design: Consecutive tumors samples accrued between 1/2009 and 2/2010 at MSKCC were analyzed for recurrent mutations in EGFR, KRAS, NRAS, HER2, BRAF, PIK3CA, AKT1 and MAP2K1 using a combination of methods including standard Sanger sequencing, fragment analysis and mass spectrometry genotyping (Sequenom) assays. Cases negative for EGFR, KRAS and BRAF were subsequently tested for EGFR exon 20 insertions and HER2 exon 20 insertions (by fragment analysis) and EML4-ALK fusions by fluorescent in-situ hybridization.

Results: A total of 1131 specimens were analyzed for all mutations. Of these, 845 were from former/current smokers and 286 from non-smokers; 719 females and 411 males. KRAS mutations were found in 358 tumors (32%), 256 (23%) harbored EGFR mutations, 16 (1.4%) BRAF, 3 (0.2%) AKT, 20 (18%) PIK3CA, 5 (0.4%) NRAS and 20 (1.8%) HER2 mutations. Of all cases tested by FISH for evidence of the EML4-ALK fusion, 40 were positive (8%). The estimated overall rate of 4%. With the exception of PIK3CA mutations and the EGFR T790M secondary mutation, all mutations concurrently tested were mutually exclusive. In all, 718/1131 tumors (63%) harbored a mutation.

Conclusions: To our knowledge, this study represents the largest comprehensive analysis of recurrent oncogenic mutations in lung adenocarcinoma. Prospective testing of lung adenocarcinomas can identify targetable oncogenic mutations in over 60% of samples which may help assign specific kinase inhibitors or aid in the further management of these patients.